ISIJ International, Vol. 44 (2004), No. 4, pp. 731–736

Impact Properties of Thin Wall Ductile Iron

Martín CALDERA, Juan Miguel MASSONE,[1)] Roberto Enrique BOERI[1)] and Jorge Antonio SIKORA[1)]

Graduate Student, Metallurgy Division, INTEMA-UNMDP-CONICET, Av. Juan B. Justo 4302 (B7608FDQ) Mar del Plata, Argentina. 1) Faculty of Engineering, División Metalurgia INTEMA, National University of Mar del Plata, CONICET, Av. Juan B. Justo 4302 (B7608FDQ) Mar del Plata, Argentina.

(*Received on October 21, 2003; accepted in final form on December 25, 2003*)

This work studies the impact strength of thin wall ductile iron. The properties of thin wall plates cast on sand moulds of thickness ranging from 2 to 4 mm, in which nodule counts ranging from 1 700 to 1 300 nod/mm^2 are measured and compared to properties obtained on samples taken from 13 and 25 mm Y blocks (ASTM A395), in which regular nodule counts are about 200 nod/mm^2. Since standard Charpy specimens could not be machined from the thin plates, some complementary studies were necessary. Impact testing of ductile iron samples of regular nodule count and different widths, showed that the resilience increases noticeably and the ductile–brittle transition temperature drops as the width diminishes. The increase in the nodule count causes a significant decrease in upper shelf resilience, and a decrease in the ductile–brittle transition temperature. Very high nodule count ferritic ductile iron, of nodule count between 1 300 and 1 700 nod/mm^2, shows a ductile–brittle transition temperature of approximately −80°C and upper shelf resilience of about 16 J/cm^2. A ductile iron of similar chemical composition, but of regular nodule count, shows a transition temperature of approximately −26°C and upper shelf resilience of approximately 18 J/cm^2.

KEY WORDS: thin wall; ductile iron; impact strength; nodule count.

1. Introduction

Ductile iron (DI) is a high strength–low cost cast material, that can be heat treated to reach a wide range of mechanical properties. Its production is commonly limited to parts of thickness greater than 5 mm. Nevertheless, its field of application could be significantly enlarged by developing the necessary technology to produce cast parts of thickness down to 2 mm. Significant research efforts are being currently devoted to the study of the production and properties of thin wall ductile iron (TWDI) parts.[1–4)] Most studies have aimed to identify the conditions to produce sound thin wall parts. This has been done by improving mould filling through a careful design of the feeding system, and by adjusting the chemical composition of the melt.[4–6)] Recent studies have proven that TWDI can reach similar tensile properties than those found in regular thickness irons.[6–10)] Nevertheless, impact properties of TWDI have not been studied yet, nor have transition temperatures been determined, to the best of our knowledge. These properties are of great importance for engineers willing to design light high-strength parts using TWDI.

Figure 1 shows impact strength *vs.* temperature for DI samples taken from parts of regular thickness (10 to 75 mm) solidified on sand moulds, that show nodule counts of 100 and 300. It is shown that the upper shelf energy drops as the nodule count increases. Meanwhile, the transition temperature diminishes as the nodule count increases.[11)] TWDI can reach nodule counts exceeding 1 500,[10)] well above the counts of regular thickness DI. The influence of such large counts on impact strength is unknown. Labrecque *et al.*,[3)] and Davis *et al.*[12)] measured impact strength of samples of as-cast DI taken from sand cast plates of 3, 10 and 12 mm thickness. The resilience (the energy for fracture divided by the initial area of the fractured section) was significantly lower for the thinner samples. Nevertheless, their results are not conclusive, since thick and thin samples had different microstructure as a result of the different cooling rates during solidification. Therefore,

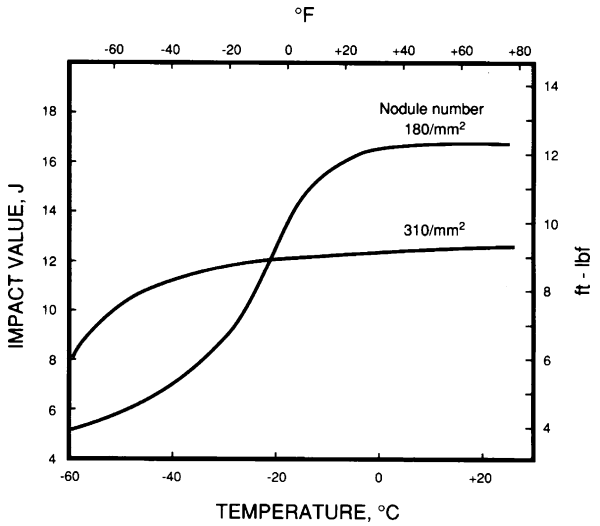

Fig. 1. Fracture energy *vs.* temperature for DI of different nodule counts.[11)]

the decrease in resilience is most probably caused by the larger amount of pearlite in the matrix. With this methodology the influence of other factors, such as the nodule count, are obscured and can not be assessed.

The objectives of the present study are to measure the impact strength of high nodule count TWDI, to identify the ductile–brittle transition temperature, to analyse the influence of nodule count on the impact strength and the transition temperature, and to assess the influence of impact sample thickness and notch on the energy absorbed on fracture.

2. Experimental Methods

2.1. Melts

The studies were carried out using three melts produced at the pilot plant of INTEMA, using a 50 kg medium frequency induction furnace. The furnace was charged using regular charge materials and ferroalloys, including graphite as re-carburiser, and (75%)FeSi. The melt was heated to 1 540°C and maintained at this temperature by 10 min before pouring. The melt was treated using Fe–Si–Mg(6%) and the sandwich method. The inoculation with Fe–Si was carried out in a separate ladle, using (75%)FeSi. **Table 1** shows the chemical composition of the melts.

2.2. Moulds and Models

Four castings were produced using melt A. The casting, shown in **Fig. 2**, has two 100×60 mm plates of 2 and 4 mm thickness.

Melt B was used to pour two Y-blocks of 25 mm and three of 13 mm. Melt C was used to pour four Y-blocks of 13 mm.

Castings were heat treated before cutting and machining the test samples. Heat treatment aimed to dissolve any ledeburitic carbide that may have formed as a result of the relatively fast cooling during solidification. The heat treatment also aimed to generate an homogeneous ferritic matrix. Ferritising was carried out by austenitising at 920°C by 1 h, followed by furnace cooling to 400°C.

Table 1. Chemical composition of the irons.

MELT	Chemical Composition (%)						
	C	Si	Mn	S	P	Mg	C.E.
A	3.60	3.02	0.23	0.02	0.04	0.04	4.60
B	3.40	3.00	0.24	0.01	0.03	0.05	4.40
C	3.50	3.07	0.15	0.017	0.04	0.051	4.52

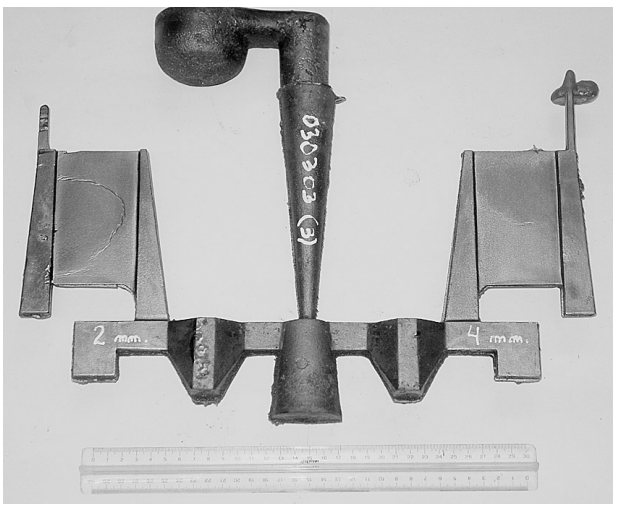

Fig. 2. Casting with thin plates.

2.3. Test Samples

The normalised shape and dimensions of Charpy test samples is shown in **Fig. 3** (ASTM E23-94b). Width values considered by the standard are 10, 7.5, 5 and 2.5 mm. This investigation uses cast plates of thickness different from the normalised width values, making it necessary to apply non-standardised samples. The impact samples where machined from the plates and blocks. The sample surface was ground (rectified). This was particularly important for the samples taken from the plates, since it involved the removal of the casting skin. The dimensions of the samples follow the definitions in ASTM E23-94b "Charpy Subsize Type A", with the exception of the width "W". Both "v-notched" and "unnotched" samples were prepared and tested. Subsize tensile test samples (ASTM E 8M Subsize Specimen) were machined from the 2 and 4 mm plates of melt A.

The nodule count and matrix microstructure were evaluated by optical microscopy. Nodule counts reported are the average of ten readings carried out by using a routine developed for the software Image Pro Plus. The software was calibrated by analysing the standard AFS charts of nodule counts.

Figure 4 shows schematically the way in which the plates were cut to obtain the impact samples. Samples taken

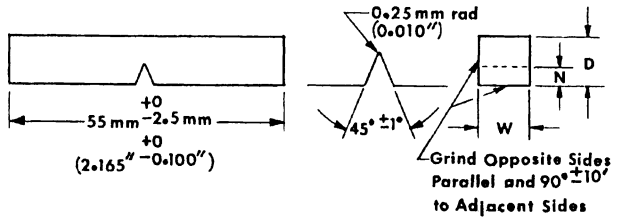

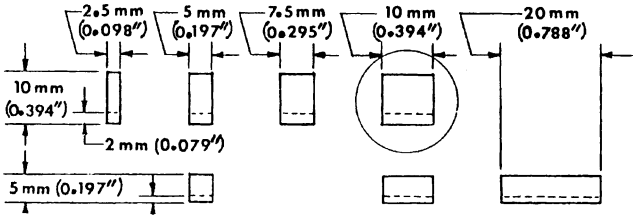

Fig. 3. Normalised shape and dimensions of Charpy test samples (ASTM E23-94b).

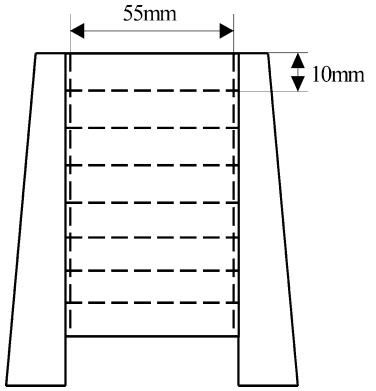

Fig. 4. Schematic of the cutting of the thin wall plates.

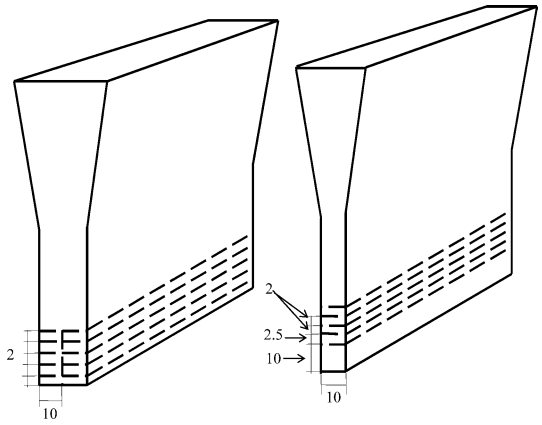

Fig. 5. Sectioning of Y-blocks of melts B and C.

Table 2. Tensile properties and nodule counts.

Melt		UTS (Mpa)	Elongation (%)	Nodule Count (nod/mm^2)
A	Thickness 2mm	462	21	1700
	Thickness 4mm	447	19.5	1300
B	Y-block, 13 mm	-	-	390
	Y-block, 25 mm	-	-	220
C	Y-block, 13 mm	-	-	330

from the 2 mm plates have a final width of 1.6 mm after surface grinding. The samples taken from the 4 mm plates were machined down to 2 mm.

The Y-blocks of melts B and C were sectioned as shown in **Fig. 5**, to obtain impact test samples of 2, 2.5, 3.5, 5, 7 and 10 mm of width.

In order to analyse the effect of the notch on the subsize impact strength, both notched and un-notched samples of 2 mm width were machined from a 13 mm Y-block of melt B.

2.4. Impact Testing

Impact tests were carried out using a pendulum Wolpert-Lestor PW5 of 50 J. Test temperatures used ranged from +45°C to −75°C. Resilience values are reported in J/cm^2, and are calculated as the energy used during the fracture divided by the initial section area fractured. Reported values at each temperature are the average of four tests. The ductile–brittle transition temperature was determined as the temperature at which the energy drops to half of the upper shelf value.

3. Results and Discussion

3.1. Metallographic Characterization and Tensile Properties

Tensile properties were only measured on the thin wall samples of Melt A. **Table 2** shows the results of tensile tests and nodule counts for the different samples used. The mechanical properties are very good for ferritic irons, satisfying the requirements for grades 60/40/18 of ASTM A 536. **Figure 6** shows the microstructure of samples of several nodule counts. The matrix microstructure is fully ferritic in all cases.

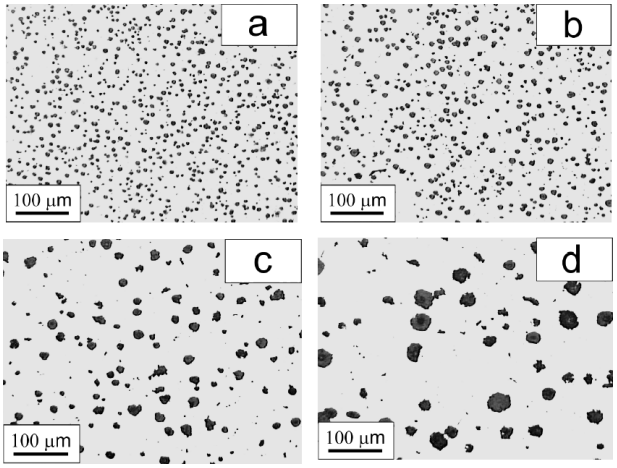

Fig. 6. Microstructure (100X) of samples of different nodule count, (a) 1 700 nod/mm^2, (b) 1 300 nod/mm^2, (c) 390 nod/mm^2, (d) 220 nod/mm^2.

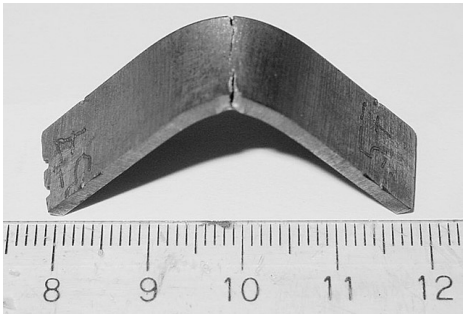

Fig. 7. Un-notched impact sample of 2 mm bent after testing. Note that un-notched samples were not used in the study since they do not give reliable results on thin specimens.

3.2. Influence of the Sample Shape and Size on Impact Properties

The first set of impact tests were carried out on un-notched samples. The results gave very scattered results, because many samples suffered extensive bending and warping. Some samples bent extensively and did not break, as that shown in **Fig. 7**. This extensive bending is caused by an instability in the load configuration when the un-notched sample width is too small. In consequence, it was concluded that testing on thin un-notched samples is unreliable, and therefore all other tests were carried out on v-notched samples.

Figure 8 shows the change in resilience as a function of temperature of v-notched samples of different thickness machined from Y-blocks of melt C. It must be noted that all samples have the same matrix microstructure and nodule count, therefore changes in resilience are solely caused by the different width of the impact sample. The results show that the impact properties are largely affected by the test sample width. **Figure 9** shows the change in upper shelf resilience and transition temperature as a function of sample width. The ductile–brittle transition temperature changes from −26°C for the 10 mm samples, to −50°C for the 2.5 mm samples. Figure 9 also shows that the upper shelf energy of samples of identical microstructure and different thickness, taken from Y-blocks of melts B and C, increases in about 30 % as the width of the impact specimen decreases from 10 to 2.5 mm.

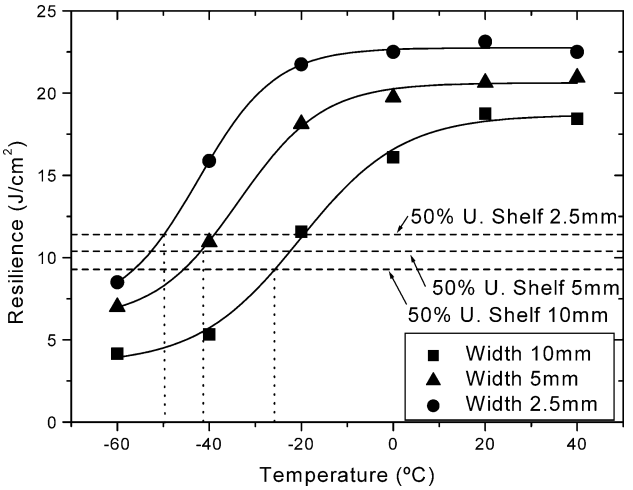

Fig. 8. Change in resilience as a function of temperature of v-notched samples of different thickness machined from Y-blocks of melt C.

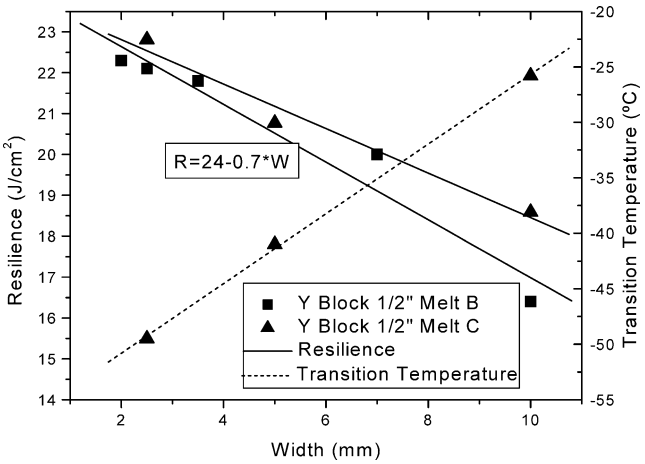

Fig. 9. Resilience [R] and transition temperature as a function of impact test sample width (W), of v-notched samples of different thickness machined from Y-blocks of melts B and C.

The large difference in resilience is accompanied by changes in the fracture surface of the samples. **Figure 10** shows the fracture surface of test samples of melt C tested at different temperatures. The samples at the bottom row show predominantly ductile fracture surface for all sample widths. As the test temperature diminishes, the surface of the samples begins to show some bright areas that indicate brittle fracture. This transition in the fracture appearance of the fracture surface takes place progressively. The 10 mm sample tested at −20°C shows some bright surface areas, while the 5 and 2.5 mm samples show much smaller amounts of brittle fracture. This is in coincidence with the resilience of those samples. In fact, at −20°C the 10 mm sample is approaching the transition temperature, while the 5 and 2.5 mm samples are still above transition. It must be noted that areas of ductile and brittle fracture are not clearly separated on the surface, but small areas of brittle and ductile fracture are finely mixed. For −60°C all samples already show completely brittle fracture.

These results confirm that neither resilience values, nor transition temperature values measured on samples of different thickness, can be compared directly. This is in coincidence with the general recommendations of ASTM Standard E 23-94b. Similar studies carried out on steel samples by K. Wallin[12] showed that the resilience of small width samples of high toughness steels is smaller than that of regular width samples. Nevertheless, as the toughness of the material tested diminishes, the resilience of small width samples turns to be larger than that of regular thickness samples. This is in coincidence with the results of the present study. The reasons for this behaviour are not clear. Transition from ductile to brittle fracture involves the transition from a ductile fracture mechanism, involving nucleation and coalescence of voids, to a brittle fracture mechanism, involving cleavage. During transition both brittle and ductile mechanisms compete. Brittle cleavage fracture must be nucleated. Nucleation sites are generally the larger critical defects or stress concentrators laying on the highly stressed portions of the samples. Considering that samples of different size are made from the same material, in the present case as the size of the sample becomes smaller, it is reasonable to assume that the size of the largest critical defects included in the stressed parts of the sample also becomes smaller. This means that brittle fracture should be able to start more easily on larger samples than on the smaller samples. This accounts for the consistently larger energy measured on the thinner samples, and the consequent drop in transition temperature.

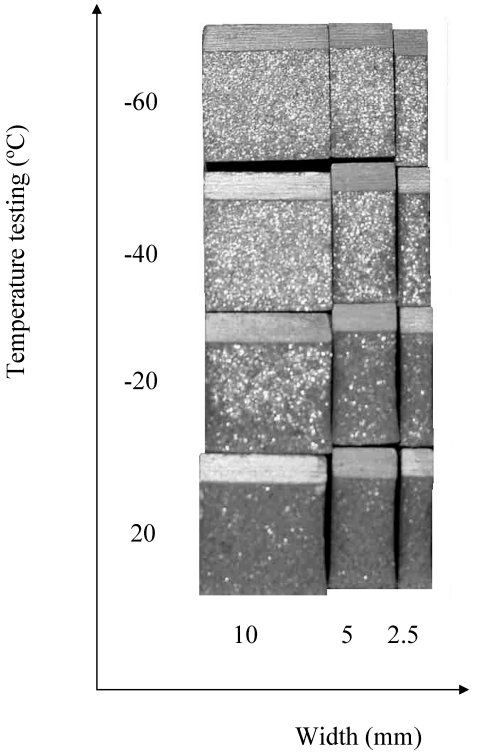

Fig. 10. Fracture surface of impact samples of melt C tested at different temperatures.

3.3. Influence of Nodule Count

Figure 11 shows the change in resilience as a function of temperature for samples of different nodule count. Each curve belongs to a set of samples of the same width. The transition temperature decreases as the nodule count increases, from approximately −45°C for the samples of 220

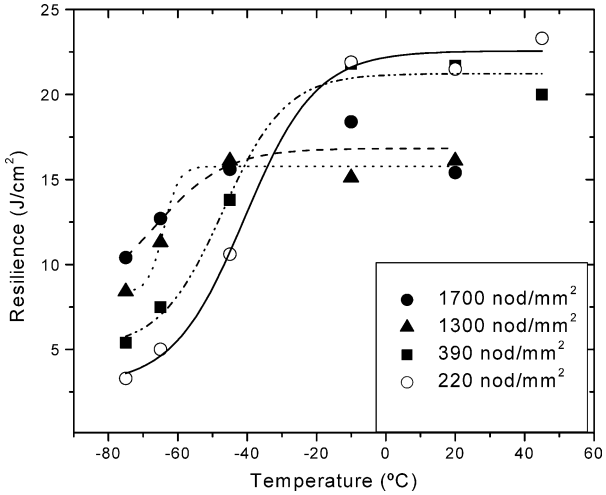

Fig. 11. Change in resilience as a function of temperature of v-notched samples of different nodule counts machined from Y-blocks and thin plates of melts A and B.

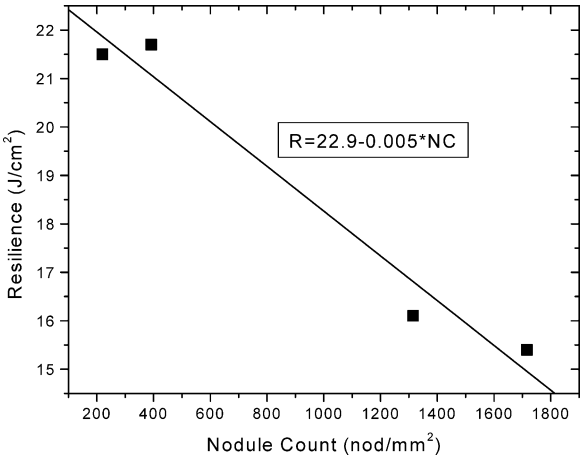

Fig. 12. Resilience in the upper shelf (20°C) as a function of nodule count.

nod/mm^2 taken from 25 mm Y-blocks, to approximately −80°C for the samples of maximum nodule count, 1 700 nod/mm^2, taken from the 2 mm thick plates. The upper shelf resilience also decrease as the nodule count increases, dropping from 22.5 to 16 J/cm^2 as the nodule count changes from 220 to 1 700. These results confirm the tendency anticipated in Fig. 1[11] for smaller nodule count irons, but show a less pronounced effect. Figure 1 showed that an increase in nodule count of 70% cause a decrease in energy of 30%, while the results of this study indicate that an increase in nodule count of 670% cause a decrease in resilience of 27%.

Figure 12 shows the resilience at 20°C as a function of nodule count, and includes an equation describing the change in room temperature resilience as a function of nodule count. **Figure 13** shows the fracture surface of thin impact samples of nodule counts of 220 and 1 700 nod/mm^2.

The fracture surface of the higher nodule count samples shows a lower proportion of brittle fracture area at a given temperature.

The influence of the nodule count on the resilience can be caused by the following effects. At the upper shelf temperatures, fracture is dominated by ductile mechanisms in-

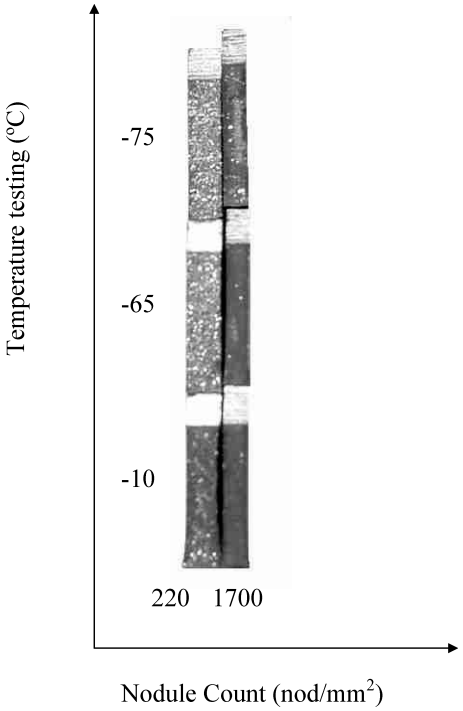

Fig. 13. Fracture surface of impact samples of melts A and B tested at different temperatures.

volving nucleation and growth of voids. Graphite particles can be considered voids, as they strength is negligible compared to that of the metallic matrix. Higher nodule count DI will therefore show larger density of nucleated voids than regular DI. This would act as if the material started to be deformed at a more advanced stage of ductile fracture, reducing the extra energy needed to cause fracture. At the lower shelf temperatures the situation is quite different. As already stated, brittle fracture is dominated by the nucleation of a cleavage fracture. As the high nodule count has solidified at a faster rate than the regular thickness irons, it microstructure is quite finer. As a result, the maximum defect size, that nucleates cleavage fracture, is smaller for the high nodule count iron, and therefore it shows an extended period of ductile fracture.

3.4. Overall Impact Properties of TWDI

This investigation has shown that TWDI of very high nodule count (>1 200 nod/mm^2) has a resilience of about 16 J/cm^2. This resilience value has been measured using impact samples of width of approximately 2 mm. Most standards require minimum impact values for ferritic ductile irons that range from 15 to 17.5 J/cm^2. A first look would indicate that the resilience values of TWDI are similar to those required for ferritic DI samples of 10 mm width and regular nodule counts. Nevertheless, this research has already shown that values measured on samples of different width are not directly comparable. The influence of the sample width can be accounted for by using the relationship shown in Fig. 9. It has shown that a small width sample has larger resilience than a 10 mm thick sample. This indicates that a 10 mm width sample of a high nodule count DI would have smaller resilience than that measured on a 2 mm sample. Nevertheless, it is not possible to verify this hypothesis since a sample of about 1 500 nod/mm^2 of

10 mm width cannot be created. As a first approximation, it can be assumed that high nodule count DI would behave like regular nodule count DI, gaining impact strength as the sample width diminishes. Under this assumption, the sample showing 16 J/cm^2 in a 1.6 mm sample would have a resilience of only 10.4 J/cm^2 if measured on a regular 10 mm width standard. This apparent lower resilience would be in part compensated when the thickness of a real part is small. Additionally, the TWDI shows a significantly lower ductile-brittle transition temperature, which may be of importance for low temperature applications.

4. Conclusions

- Impact testing of ductile iron samples of regular nodule count and different widths, showed that the resilience increases noticeably and the ductile–brittle transition temperature drops as the width diminishes. This confirms that resilience values measured on samples of different width cannot be compared directly.
- The increase in the nodule count causes a significant decrease in the upper shelf resilience, while it also causes a decrease in the ductile–brittle transition temperature.
- Very high nodule count ferritic ductile iron, of nodule count between 1 300 and 1 700 nod/mm^2, show a ductile–brittle transition temperature of approximately −80°C and an upper shelf resilience of about 16 J/cm^2. A ductile iron of similar chemical composition, but of regular nodule count, shows a transition temperature of approximately −26°C and an upper shelf resilience of approximately 18 J/cm^2, when tested using samples of 10 mm width.

REFERENCES

1) J. F. Cuttino, J. R. Andrews and T. S Piwonka: *AFS Trans.*, **107** (1999), 363.
2) A. Javaid, J. Thomson, M. Sahoo and K. G. Davis: *AFS Trans.*, **107** (1999), 441.
3) C. Labrecque, M. Gagne, A. Javaid and M. Sahoo: *Int. J. Cast Metals Research*, **16** (2003), 313.
4) F. Mampaey and Z.A. Xu: *AFS Trans.*, **105** (1997), 95.
5) M. Caldera, J. Massone, R. Boeri and J. Sikora: Proc. SAM-CONAMET-AAS 2001, ed. by Universidad Nacional de Misiones, Posadas, Argentina, (2001), 75.
6) D. M Stefanescu, L. P. Dix, R. E. Ruxanda, C. Corbitt-Coburn and T. S. Piwonca: *AFS Trans.*, **110** (2002), 1149.
7) L. P. Dix, R. Ruxanda, J. Torrance, M. Fukumoto and D. M. Stefanescu: *AFS Trans.*, **111** (2003), 109.
8) A. Javaid, K. G. Davis and M. Sahoo: *AFS Trans.*, **108** (2000), 191.
9) D. M. Stefanescu, R. Ruxanda and L. P. Dix: *Int. J. Cast Metals Research*, **16** (2003), 319.
10) D. Novelli, J. Massone, R. Boeri and J. Sikora: Proc. CONAMET/SAM SIMPOSIO MATERIA 2002, ed. by Ediciones y Representaciones Tecnicas Ltda., Santiago, Chile, (2002), 163.
11) Ductile Iron Data for Design Engineers, ed. by QIT-Fer et Titane Inc, Sorel, Canada, (1990), 3.
12) K. Wallin: *Int. J. Pressure Vessels Piping*, **78** (2001), 463.